Nanoparticle Adsorption

DOI: 10.1002/anie.201405317

Langmuir Analysis of Nanoparticle Polyvalency in DNA-Mediated Adsorption**

*Matthew N. O'Brien, Boya Radha, Keith A. Brown, Matthew R. Jones, and Chad A. Mirkin**

Abstract: *Many nanoparticle adsorption processes are dictated by the collective interactions of surface-bound ligands. These adsorption processes define how nanoparticles interact with biological systems and enable the assembly of nanoparticle-based materials and devices. Herein, we present an approach for quantifying nanoparticle adsorption thermodynamics in a manner that satisfies the assumptions of the Langmuir model. Using this approach, we study the DNA-mediated adsorption of polyvalent anisotropic nanoparticles on surfaces and explore how deviations from model assumptions influence adsorption thermodynamics. Importantly, when combined with a solution-based van't Hoff analysis, we find that polyvalency plays a more important role as the individual interactions become weaker. Furthermore, we find that the free energy of anisotropic nanoparticle adsorption is consistent across multiple shapes and sizes of nanoparticles based on the surface area of the interacting facet.*

Molecular adsorption models are used to quantify surface coverage of molecular species, to characterize adsorption kinetics, and to evaluate the interaction thermodynamics between a molecular adsorbate and a surface site on an adsorbent. The most common molecular-adsorption model, the Langmuir model, uses equilibrium adsorption and desorption rate equations to relate the bulk concentration or pressure of an adsorbate to the percentage of occupied surface sites on an adsorbent, and thereby calculate an equilibrium adsorption constant.[1] Despite the simplicity of the Langmuir model, and accordingly the large number of implicit assumptions, this model accurately describes many adsorption processes. Consequently, Langmuir isotherm analyses have found use in a variety of fields, the foremost being heterogeneous catalysis, where they are used as a standard tool for catalyst design and optimization.[2] More recently, the Langmuir model has been applied to ligand adsorption on nanoparticle adsorbents in solution as a means to quantify surface saturation and ligand affinity.[3]

In contrast to molecular adsorption, nanoparticle adsorption processes can be very complicated and difficult to understand, as interactions between nanoparticles and surfaces are dictated by the collective behavior of many attached ligands, rather than a single connection, and surface sites are no longer atomically defined. The thermodynamics of polyvalent interactions are dictated by the density, proximity, and arrangement of the individual ligands, and therefore determination of the collective interaction strength is often not as simple as summing the number of individual interactions.[4] Accordingly, to correctly describe nanoparticle adsorption with models initially intended for simple molecular systems requires careful attention to the model assumptions. Several groups have attempted to use a Langmuir model to describe nanoparticle adsorption; however, deviation from Langmuir assumptions (such as the failure to account for adsorption reversibility and/or the effect of adsorbate–adsorbate interactions) may negate extraction of thermodynamic parameters.[5] Alternatively, complementary polyvalent interactions between nanoparticles in solution have been well-studied as a function of both nanoparticle and ligand properties.[6] However, it is not clear to what extent these findings can be extended to analogous surface-based adsorption events. The development of a model system to study nanoparticle adsorption processes, where non-ideal adsorption behavior and the difference between surface and solution-based measurements can be investigated, is therefore of fundamental importance to understand how polyvalency has an impact on the interaction of nanoparticles with biological environments[7] and to engineer nanoparticle-based materials and devices.[8]

Herein, we report a model system to study nanoparticle adsorption processes that satisfies the assumptions of the Langmuir model. This approach is used to study the adsorption of polyvalent DNA-functionalized anisotropic noble metal nanoparticles to lithographically-defined surface

[*] M. N. O'Brien,[+] Dr. B. Radha,[+] Dr. K. A. Brown, Prof. C. A. Mirkin
Department of Chemistry
International Institute for Nanotechnology
Northwestern University
2145 Sheridan Rd, Evanston, IL 60208 (USA)
E-mail: chadnano@northwestern.edu
M. R. Jones, Prof. C. A. Mirkin
Department of Materials Science and Engineering
Northwestern University
2220 Campus Dr., Evanston, IL 60208 (USA)
[+] These authors contributed equally to this work.

[**] This material is based upon work supported by the following awards: AFOSR FA9550-11-1-0275, AFOSR FA9550-12-1-0280, and NSF DMR-1121262 at the Materials Research Center of Northwestern University. This work made use of the EPIC facility (NUANCE Center-Northwestern University), which has received support from the MRSEC program (NSF DMR-1121262) at the Materials Research Center, and the Nanoscale Science and Engineering Center (EEC-0118025/003), both programs of the National Science Foundation; the State of Illinois; and Northwestern University. M.N.O. acknowledges the NSF for a Graduate Research Fellowship. B.R. acknowledges an Indo-US postdoctoral fellowship. M.R.J. acknowledges the NSF for a Graduate Research Fellowship and Northwestern University for a Ryan Fellowship. K.A.B. acknowledges support from Northwestern University's International Institute for Nanotechnology.

Supporting information for this article is available on the WWW under http://dx.doi.org/10.1002/anie.201405317.

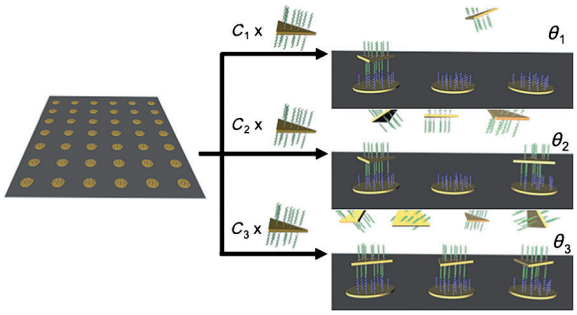

Scheme 1. The model system for nanoparticle-based Langmuir adsorption mediated by complementary DNA hybridization events. Lithographically defined surface sites functionalized with DNA represent the adsorbent, while DNA-functionalized triangular prisms represent the adsorbates. The concentration (c) of adsorbates in solution determines the fraction (θ) of surface sites that are occupied. Note: DNA is not to scale.

sites functionalized with complementary DNA (Scheme 1). Using this system, we quantify the free energy of adsorption and report how deviations from the assumptions of the Langmuir model can influence binding constants by more than an order of magnitude. We then compare the free energy of nanoparticle adsorption onto surfaces to analogous DNA-mediated nanoparticle–nanoparticle interactions in solution. Interestingly, we find that the importance of interaction polyvalency increases with increasing temperature. We conclude by showing that the measured free energy of adsorption of five different faceted nanoparticles have a consistent relationship with the surface area of their interacting facets.

To provide a tunable interaction between nanoparticles and a surface, we utilized complementary DNA hybridization interactions (Figure S2 in the Supporting Information). In particular, lithographically-defined gold surface sites and gold nanoparticles were densely functionalized with unique thiolated, single-stranded oligonucleotides that were subsequently hybridized with a complementary "linker" strand. The linker strand had a five-base terminus designed to link the nanoparticle to the surface through complementary DNA interactions. Although individual DNA hybridization events linking the nanoparticle to the surface were designed to be weak, the collective interaction of many strands on a nanoparticle interacting with complementary strands on the surface governs nanoparticle adsorption. Several studies on the hybridization thermodynamics of such collective interactions have been performed for complementary particle interactions in extended aggregate systems.[6a,c,e,f,9] These studies have demonstrated the importance of particle size, DNA density, and DNA sequence in the context of spherical particles, where a greater number of DNA hybridization events linking particles leads to a more negative free energy of association. This difference in free energy has been exploited to separate nanoparticles of different sizes through a temperature-dependent selective crystallization process.[10] More recently, the role of shape was investigated through comparison of spheres and triangular prisms with similar numbers of DNA strands in which the triangular prisms exhibited a binding constant that was enhanced by six orders of magnitude.[6c] This result was attributed to several factors, including the greater number of hybridization events that may occur between triangular prisms as a result of the commensurate alignment of the DNA ligands on the atomically flat triangular facets. While these studies have elucidated many of the foundational principles for DNA-mediated nanoparticle assembly, systematic investigation of anisotropic nanoparticle hybridization thermodynamics as a function of particle size and shape has yet to be undertaken and there have been no studies of single anisotropic nanoparticle adsorption events.

Therefore, we hypothesized that investigating the interaction between a single nanoparticle and a surface could provide insight into the role of polyvalency in nanoparticle adsorption without the complications associated with lattice formation. In a typical nanoparticle adsorption experiment, substrates with DNA-functionalized surface sites were immersed in solutions of nanoparticles functionalized with complementary DNA strands over a range of nanoparticle concentrations (Scheme 1). Importantly, the DNA sequences used resulted in an approximately 20 nm spacing between the nanoparticle and the surface, a distance where DNA hybridization should be the dominant force driving nanoparticle adsorption as opposed to substrate–particle interactions. The substrates were then dried[11] and the surface occupancy was measured by counting the fraction of surface sites with adsorbed nanoparticles (from SEM images) for statistical numbers of surface sites. A fit to surface occupancy versus nanoparticle concentration yields a characteristic Langmuir adsorption constant K_L. The Langmuir adsorption model relates surface occupancy θ and concentration c to the rates of adsorption and desorption at equilibrium through Equation (1):

$$c\,(1-\theta)\,k_a = \theta k_d \tag{1}$$

where k_a is the adsorption rate constant and k_d is the desorption rate constant. Substituting $K_L = k_a/k_d$ and rearranging for θ yields the classic Langmuir form [Eq. (2)]:

$$\theta = \frac{K_L c}{1 + K_L c} \tag{2}$$

As is apparent from the simplicity of this model, there are a number of assumptions made about the adsorption process, including (Figure 1): 1) all sites on the adsorbent have an equal probability for adsorption; 2) the adsorption of a species at one surface site does not influence the adsorption of another (that is, the enthalpy and entropy of adsorption are the same for each adsorption event and independent of surface coverage); 3) only a single adsorbate may be located per surface site (adsorption is limited to a monolayer); 4) adsorbates must be non-interacting prior to adsorption; and 5) adsorption is reversible (adsorption is an equilibrium process).

Herein, we developed a model system in which each of these assumptions can be addressed independently (Figure 1). It is interesting to note that our ability to control and characterize each assumption is difficult or impossible to achieve in molecular systems. First, to eliminate the interaction between surface sites, we utilized electron-beam

lithography to define gold features commensurate with the size of the nanoparticle that, when functionalized, capture single nanoparticles. This ensures reproducible and independent surface sites, each with an equal probability for adsorption (assumptions 1–3; Figure 1 a, b). This step eliminates in-plane nanoparticle–nanoparticle interactions by limiting adsorption to a single nanoparticle per surface site. Interestingly, we found a wide tolerance range for this step, wherein surface sites with diameters 0.9–1.1 times the nanoparticle edge length resulted in a single adsorbate per site. Second, we found that nonspecific interactions between nanoparticles in solution compete with surface adsorption at low temperatures and can result in multilayer growth (in violation of assumptions 3, 4). By elevating the reaction temperature above the dissociation temperature of these nonspecific interactions, but below the dehybridization temperature of the adsorbate–adsorbent connection, associated nanoparticles become discrete
(Figure 1 c) and surface adsorption occurs in a sequence-specific manner (Figure 1 d; assumptions 3 and 4 are satisfied). Lastly, to ensure the occupancy measurement captured a thermodynamic, rather than a kinetic state, we performed a UV/Vis absorption spectroscopy melting experiment for an analogous system to show that the nanoparticle adsorption process was reversible (assumption 5; Figure 1 e). Furthermore, we performed time-dependent adsorption experiments and selected a time point after which the system had reached equilibrium (Figure 1 f, g).

With the Langmuir model assumptions satisfied for this system, the ability to extract meaningful thermodynamic quantities was explored (Figure 2). Specifically, the adsorption of triangular prism nanoparticles onto circular surface sites commensurate with their size was studied at 40 °C. Triangular prism nanoparticles were chosen because of their high degree of anisotropy, which results in a single type of nanoparticle–surface interaction (with the atomically flat, triangular-shaped nanoparticle facet parallel to the surface) that can be approximated by the surface area of the

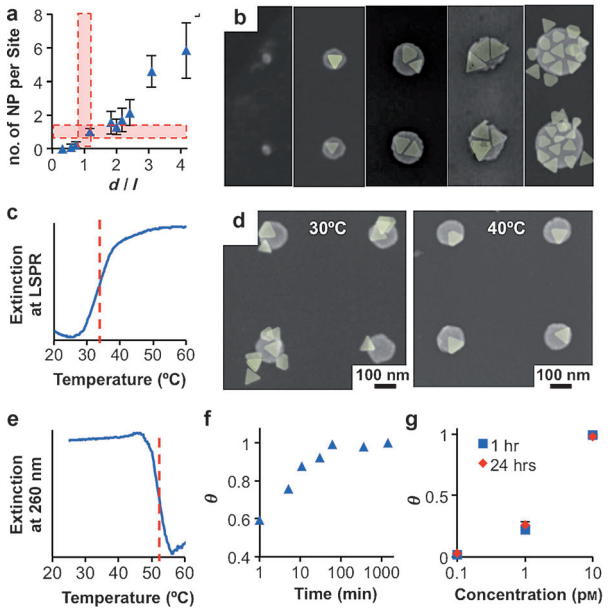

Figure 1. Addressing the assumptions of a nanoparticle-based Langmuir method. a) Plot showing the number of nanoparticles per surface site versus the parameter d/l, where l is the nanoparticle edge length and d is the diameter of the lithographically defined surface sites. By varying d with respect to l, a single nanoparticle could be adsorbed per surface site (red region). b) SEM images showing adsorption of nanoparticles onto surface sites of varying diameter to obtain a single absorbed nanoparticle per surface site. c) UV/Vis melting analysis monitoring the extinction of the nanoparticles at the localized surface plasmon resonance (LSPR) of the triangular prisms as a function of temperature. The nonspecific interactions between nanoparticles are broken apart with a transition temperature at 34 °C (red dashed line). d) SEM images showing Langmuir adsorption experiments performed below the nonspecific transition temperature (30 °C) result in multilayer adsorption. Above the transition temperature (40 °C) a monolayer is adsorbed. e) UV/Vis melting analysis monitoring the extinction at $\lambda = 260$ nm of triangular prisms hybridized to a gold film with increasing temperature. Nanoparticle adsorption is reversible with a desorption temperature of 52 °C. f) Surface-occupancy (θ) measurements for 60 nm triangular prisms at 10 pM and 40 °C as a function of adsorption time. g) Surface-occupancy (θ) measurements for 60 nm triangular prisms at 40 °C for 1 hour and 24 h at three different concentrations, showing that equilibrium is reached after one hour. Nanoparticles in images are false-colored to enhance contrast.

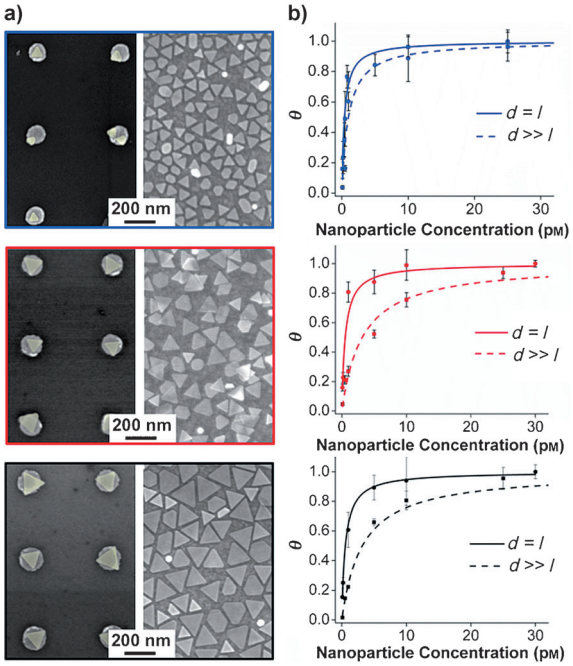

Figure 2. Investigation of deviations from Langmuir assumptions. Adsorption is compared for surface site diameter (d) to nanoparticle edge length (l) ratios: $d \approx l$ (Langmuir conditions) and $d = 10\ \mu m \gg l$ (non-Langmuir conditions). a) SEM images showing particles adsorbed under Langmuir conditions (left, particles false-colored to enhance contrast) and non-Langmuir conditions (right). b) Surface occupancy measurements for nanoparticles adsorbed under Langmuir conditions (——) and non-Langmuir conditions (-----). For the Langmuir conditions, adsorption constants of triangular prisms with edge lengths of 60 nm (blue), 100 nm (red), and 140 nm (black) were statistically similar. Adsorption constants for non-Langmuir conditions were suppressed by at least 80% for all three sizes, with the extent of suppression scaling with nanoparticle edge length.

interacting facet.[6c,12] Three different edge lengths of triangular prisms (all with the same thickness)[13] were investigated to determine trends associated with nanoparticle size, and accordingly, the number of DNA ligands that could potentially participate in nanoparticle adsorption (i.e. the polyvalency of the interaction). As predicted, the data fit well to the Langmuir form for all three nanoparticle sizes (Figure 2; Supporting Information, Figures S4–S6). Surprisingly, K_L values for the three triangular prism sizes investigated were all within error of each other (approximately $1.8 \pm 0.3 \times 10^{12}$ L mol^{-1}), which suggests that increased size (and therefore greater number of DNA molecules) did not significantly impact the thermodynamics of surface adsorption at this temperature.

To probe how a violation of the above Langmuir model assumptions effects the measurement of an adsorption constant, we compared the adsorption of nanoparticles under the Langmuir conditions described above (i.e. onto lithographically defined surface sites commensurate with the size of the nanoparticle) to the adsorption onto surface sites much greater than the size of the nanoparticles (Figure 2; Supporting Information, Figures S7–S9). This comparison allows the importance of non-interacting surface sites and in-plane particle–particle interactions in our Langmuir model to be evaluated and the cooperativity of nanoparticle adsorption to be determined under "non-Langmuir" conditions (assumption 2). Thus, the same triangular prism nanoparticles and experimental conditions were used to study adsorption onto effectively "bulk" films at 40 °C. An immediate problem became apparent for the characterization of these non-Langmuir experiments, as the surface sites were not well-defined for an explicit number of nanoparticle adsorption events, but were instead dependent on the packing density of the nanoparticles. To address this, the occupancy θ was assumed to be unity at the highest concentration tested (Supporting Information, Figure S1). With this assumption, the effective adsorption constants, $K_{L,eff}$, were measured to be suppressed by at least 80% from the Langmuir experiments and showed a statistically significant difference between the three sizes. Specifically, we found that $K_{L,eff}$ values were inversely related to nanoparticle size with 60 nm, 100 nm, and 140 nm edge length triangular prisms having $K_{L,eff}$ values of $4.6 \pm 0.1 \times 10^{11}$ L mol^{-1}, $3.3 \pm 0.1 \times 10^{11}$ L mol^{-1}, and $2.3 \pm 0.1 \times 10^{11}$ L mol^{-1}, respectively. Because K_L values for the three sizes of triangular prisms were statistically similar, we can attribute the differences in $K_{L,eff}$ to interactions between adsorbates. This suggests a negative cooperativity for nanoparticle adsorption under non-Langmuir conditions, wherein each nanoparticle adsorption event suppresses the likelihood of subsequent adsorption events. The trend of decreased $K_{L,eff}$ with increased nanoparticle size suggests a physical origin to this effect, wherein adsorbed nanoparticles decrease the surface area available for subsequent binding events in a manner commensurate with their size. There is likely an electrostatic component to this effect as well, in which the negatively charged nanoparticle adsorbates repel other nanoparticles. These results emphasize the importance of matching experimental conditions to model assumptions to accurately measure single nanoparticle thermodynamics.

Secondary methods to characterize the thermodynamics of nanoparticle adsorption onto surfaces are limited, but analogous studies can be performed for nanoparticle–nanoparticle interactions in solution using well-established methods. Although such studies can be designed to utilize the same complementary interactions that occur for nanoparticle adsorption, adsorption of nanoparticles in solution differs in three primary ways: 1) adsorption is not limited to a single adsorption event per particle, but instead results in extended aggregate systems (for example, each triangular prism may be involved in two adsorption events); 2) adsorption is between two nanoparticles, rather than a nanoparticle and a lithographically-defined feature, and thus the bound product is still free in solution; and 3) commonly used van't Hoff analysis of adsorption thermodynamics is most effective in systems with comparable populations of reactants and products, thus limiting experimentally accessible temperatures. With these differences in mind, we extracted thermodynamic parameters from the concentration dependence of the equilibrium melting temperature of triangular prism nanoparticles assembled with the same complementary DNA design (Figure 3; Supporting Information, Figure S15).[6c,14] Melting, in the context of nucleic acids, refers to the transition from a hybridized to a dehybridized state, and is performed by monitoring the absorbance at $\lambda =$ 260 nm as a function of temperature. In the context of nanoparticles connected by hybridized DNA, an analogous experiment can be performed by monitoring the nanoparticle extinction at the localized surface plasmon resonance (LSPR) as a function of temperature. In this case, a transition is detected in the LSPR in going from an aggregated state with dampened extinction at low temperatures to a dispersed nanoparticle state with an enhanced extinction at high temperatures. The reverse of this experiment, from high to

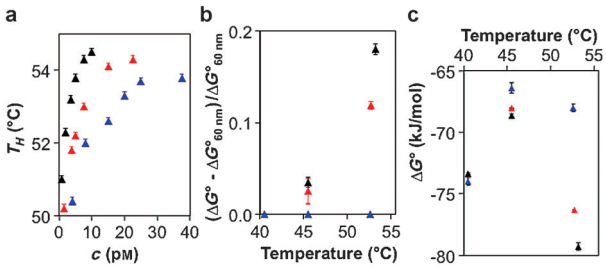

Figure 3. Nanoparticle–surface interactions measured with the Langmuir model compared to analogous nanoparticle–nanoparticle interactions in solution. a) Concentration (c) dependence of the equilibrium hybridization temperature (T_H) measured for 60 nm (blue), 100 nm (red), and 140 nm (black) triangular prisms. b) $\Delta G°$ was calculated from a van't Hoff analysis of the data in (a) and plotted with Langmuir data collected at two temperatures (40 and 45 °C). The data are plotted by using the $\Delta G°$ of the smallest triangular prism ($\Delta G°_{60\,nm}$) as a reference to show the effect of polyvalency with increasing nanoparticle size. The change in $\Delta G°$ with respect to $\Delta G°_{60\,nm}$ was then normalized with respect to $\Delta G°_{60\,nm}$ to account for the relative magnitude of the change. Van't Hoff data is plotted at the median temperature for the data given in (a). c) Absolute values of $\Delta G°$ in (b) were used to show the difference in magnitude of $\Delta G°$ for the two techniques.

low temperatures, measures hybridization, rather than dehybridization. Van't Hoff analysis can be used to relate the concentration dependence of this transition to enthalpy $\Delta H°$ and entropy $\Delta S°$ through Equation (3):

$$\frac{1}{T_m} = \frac{R}{\Delta H^\circ}\ln(c) + \frac{[\Delta S^\circ - R\ln(4)]}{\Delta H^\circ} \quad (3)$$

where T_m represents the equilibrium melting temperature and R represents the ideal gas constant.

From this analysis, we find that both $\Delta H°$ and $\Delta S°$ become more negative with increasing triangular prism edge length (Supporting Information, Table S2). A more negative $\Delta H°$ suggests that a greater number of DNA ligands engage in hybridization as the nanoparticle size increases, while a more negative $\Delta S°$ implies an entropic penalty for the transition from dehybridized to hybridized states that scales with the number of DNA ligands. However, it is worth noting that T_m for the three triangular prism sizes differed less than 3 °C at each concentration measured, a much smaller change than that measured for spheres of analogous diameters (> 9 °C).[9b] Furthermore, the measured differences in enthalpy and free energy were orders of magnitude smaller than would be expected based upon the additional number of DNA strands. These data suggest that a greater degree of polyvalency, and therefore a greater number of hybridization events linking nanoparticles, correlates to a stronger binding strength between nanoparticles. However, this occurs in a negatively cooperative manner (i.e. each subsequent binding event is weaker than the previous binding event)[4a] and to a lesser extent than for spherical particles. We hypothesize that the difference in hybridization behavior for spheres and triangular prisms as a function of size can be attributed to radius-of-curvature effects. As the sphere transitions from a highly curved to an effectively "flat" surface from small to large nanoparticle diameters, a greater number of hybridization events can occur.[6c] In contrast, the triangular prisms only change in edge length, and retain a constant shape.

The free energy of solution-based nanoparticle association can be related to Langmuir data collected for multiple temperatures, using Equations (4) and (5):

$$\Delta G^\circ = \Delta H^\circ - T\Delta S^\circ \quad (4)$$

and

$$\Delta G^\circ = -R\,T\ln K_L \quad (5)$$

where $\Delta G°$ is the change in Gibb's free energy of adsorption. As shown in the Langmuir measurements, $\Delta G°$ was found to increase with increasing temperature. Two notable differences were evident between the surface-based and the solution-based measurements of adsorption thermodynamics. First, the surface-based data showed an unexpected minimal variation of $\Delta G°$ with nanoparticle size (less than 0.1 kJ mol^{-1}) at 40 °C and a more anticipated decrease (greater than 0.7 kJ mol^{-1}) in $\Delta G°$ with increasing size at 45 °C. In comparison, the solution-based analysis showed a difference of more than 5 kJ mol^{-1} between each of the sizes. Second, $\Delta G°$ was found to be 8–16 kJ mol^{-1} lower by the surface-based measurements for all three triangular prism sizes, which, given the similarity between their slopes with respect to temperature, is primarily related to a more positive $\Delta H°$ (Figure 3b; Supporting Information, Table S2, Figure S10–S12).

To explain the observed trends in adsorption free energy as a function of nanoparticle size for the two techniques utilized, it is instructive to compare the temperature range of each experiment. The Langmuir experiments necessarily are carried out below the desorption temperature such that a measurable number of surface sites are occupied. In contrast, the solution-based nanoparticle association experiments can only directly measure the desorption temperature, with extrapolation required above or below this temperature. However, extrapolation assumes that $\Delta H°$ values and $\Delta S°$ values are invariant to temperature, and therefore this analysis is most valid across the range of transition temperatures measured. When combined, the solution-based and surface-based experiments allow us to measure hybridization thermodynamics across a wide range of temperatures, and together, we observe an increasing dependence on nanoparticle size with increasing temperature. This trend can be explained by the polyvalency of the nanoparticle. At low temperatures, the strength of an individual hybridization event is relatively large, and therefore fewer linkages dictate adsorption. As the temperature increases, the strength of an individual hybridization event weakens, and therefore adsorption behavior is dictated by the collective behavior of many weak linkages. Accordingly, triangular prisms with a greater number of DNA linkers exhibit an increased association strength at high temperatures, but behave similarly to triangular prisms with fewer DNA linkers at low temperatures.

Although the above discussion contextualizes the trends in free energy measured with each technique, it does not explain the difference in the magnitude of adsorption free energy. If we assume that the enthalpy of any individual hybridization event is the same whether it happens between particles or between a particle and a surface, these data suggest that fewer DNA connections form between the substrate and the nanoparticle compared to the nanoparticle–nanoparticle case. One potential explanation could be the greater surface roughness of the lithographically defined surface sites (approximately 0.5 nm peak-to-peak surface roughness on the surface; Supporting Information, Figure S16) as compared to the atomically flat triangular prisms. This surface roughness likely limits the number of hybridization events that can occur between the nanoparticle and the surface or introduces a greater degree of strain into these interactions. Additionally, adsorption may be enhanced in the solution measurement, as each triangular prism can participate in two adsorption events compared to the single nanoparticle–surface adsorption event. This suggests that solution-based measurement of nanoparticle–nanoparticle association thermodynamics can be used to estimate the trends in single nanoparticle adsorption behavior for differently sized nanoparticles, however, this may not be appropriate to measure the magnitude of adsorption free energy.

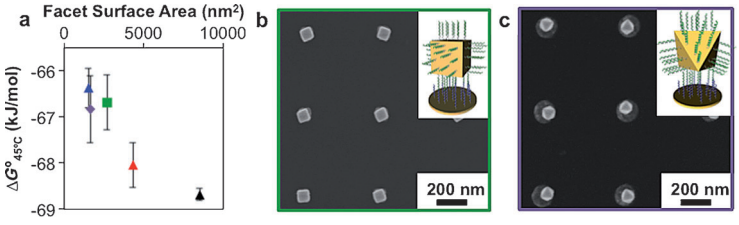

Figure 4. Langmuir adsorption isotherms for five different faceted anisotropic nanoparticles as a function of shape and size. a) Free energy of adsorption measurements at 45 °C ($\Delta G°_{45°C}$) for these five nanoparticles show agreement with each other. Each nanoparticle species is represented by a point with a specific color and shape to indicate size and shape, respectively. Colors correspond to data displayed in Figures 2 and 3 for clarification. b), c) Representative SEM images at high occupancy for 52 nm edge length cubes (green; b) and 62 nm edge length octahedra (purple; c). Note: DNA not to scale.

Although we have focused on triangular prism nanoparticles, the relationship between temperature and polyvalency should be generalizable to any faceted nanoparticle. Langmuir isotherms were measured at 45 °C for two other nanoparticle shapes: cubes and octahedra, with facet surface areas between that of the 60 and 100 nm triangular prisms (Figure 4; Supporting Information, Figure S13–S15). These experiments were enabled by recent measurement of nanoparticle extinction coefficients as a function of size and shape.[15] Importantly, this analysis resulted in K_L values between those measured for the 60 nm and 100 nm triangular prisms, suggesting that the approach and results described herein could be generalized to an arbitrary anisotropic nanoparticle with flat facets within the range of facet surface areas investigated (Supporting Information, Table S2). Facet surface areas smaller than those investigated herein and nanoparticle surface curvature may result in deviations from this behavior and therefore warrant further investigation.

In summary, we have developed a nanoparticle-based Langmuir adsorption model, in which the adsorption thermodynamics for DNA-functionalized anisotropic nanoparticles can be measured and understood in the context of polyvalent interactions. In particular, we have shown that the number of individual interactions connecting a nanoparticle and a surface (i.e. the polyvalency of the interaction) plays an increasingly important role in adsorption as the strength of each individual interaction is decreased. Furthermore, we have found that the free energy of nanoparticle adsorption increases with the polyvalency of the nanoparticle, however, the free energy of each individual connection appears to decrease as polyvalency increases. These insights suggest a positive polyvalent cooperativity, but a negative cooperativity with respect to each successive individual connection.[4a] Finally, these results enable the adsorption of multiple nanoparticle shapes and sizes in a predictable manner. We imagine this model could be extended to other complementary ligand interactions beyond DNA to evaluate the interactions between nanoparticles and biological systems as a function of ligand number and ligand density, as well as the ligand orientation and arrangement templated by the nanoparticle. Such results could be used to better understand and engineer how biomolecule-functionalized nanoparticles interact with their environment for in vitro and in vivo applications.

Received: May 15, 2014
Published online: July 13, 2014

Keywords: adsorption · DNA · Langmuir model · nanoparticles · polyvalency

[1] I. Langmuir, *J. Am. Chem. Soc.* **1918**, *40*, 1361 – 1403.
[2] L. Gaines George, G. Wise in *Heterogeneous Catalysis*, *Vol. 222*, American Chemical Society, Washington, DC, **1983**, pp. 13 – 22.
[3] a) H. Zhang, R. L. Penn, R. J. Hamers, J. F. Banfield, *J. Phys. Chem. B* **1999**, *103*, 4656 – 4662; b) S. H. Brewer, W. R. Glomm, M. C. Johnson, M. K. Knag, S. Franzen, *Langmuir* **2005**, *21*, 9303 – 9307; c) O. F. Odio, L. Lartundo-Rojas, P. Santiago-Jacinto, R. Martínez, E. Reguera, *J. Phys. Chem. C* **2014**, *118*, 2776 – 2791; d) Y. Wang, A. Neyman, E. Arkhangelsky, V. Gitis, L. Meshi, I. A. Weinstock, *J. Am. Chem. Soc.* **2009**, *131*, 17412 – 17422; e) W. R. Glomm, Ø. Halskau, A.-M. D. Hanneseth, S. Volden, *J. Phys. Chem. B* **2007**, *111*, 14329 – 14345.
[4] a) M. Mammen, S.-K. Choi, G. M. Whitesides, *Angew. Chem. Int. Ed.* **1998**, *37*, 2754 – 2794; *Angew. Chem.* **1998**, *110*, 2908 – 2953; b) C. A. Hunter, H. L. Anderson, *Angew. Chem. Int. Ed.* **2009**, *48*, 7488 – 7499; *Angew. Chem.* **2009**, *121*, 7624 – 7636.
[5] a) C. Wilhelm, F. Gazeau, J. Roger, J. N. Pons, J. C. Bacri, *Langmuir* **2002**, *18*, 8148 – 8155; b) J. J. Park, S. H. D. P. Lacerda, S. K. Stanley, B. M. Vogel, S. Kim, J. F. Douglas, D. Raghavan, A. Karim, *Langmuir* **2009**, *25*, 443 – 450; c) K. Fujiwara, H. Kasaya, N. Ogawa, *Anal. Sci.* **2009**, *25*, 241 – 248; d) R. P. Carney, Y. Astier, T. M. Carney, K. Voïtchovsky, P. H. Jacob Silva, F. Stellacci, *ACS Nano* **2013**, *7*, 932 – 942; e) P. Wagener, A. Schwenke, S. Barcikowski, *Langmuir* **2012**, *28*, 6132 – 6140.
[6] a) R. Jin, G. Wu, Z. Li, C. A. Mirkin, G. C. Schatz, *J. Am. Chem. Soc.* **2003**, *125*, 1643 – 1654; b) K. J. M. Bishop, C. E. Wilmer, S. Soh, B. A. Grzybowski, *Small* **2009**, *5*, 1600 – 1630; c) M. R. Jones, R. J. Macfarlane, A. E. Prigodich, P. C. Patel, C. A. Mirkin, *J. Am. Chem. Soc.* **2011**, *133*, 18865 – 18869; d) F. Li, D. P. Josephson, A. Stein, *Angew. Chem. Int. Ed.* **2011**, *50*, 360 – 388; *Angew. Chem.* **2011**, *123*, 378 – 409; e) S. Y. Park, D. Stroud, *Phys. Rev. B* **2003**, *67*, 212202; f) R. Dreyfus, M. E. Leunissen, R. Sha, A. V. Tkachenko, N. C. Seeman, D. J. Pine, P. M. Chaikin, *Phys. Rev. Lett.* **2009**, *102*, 048301; g) X. C. Ye, J. Chen, M. Engel, J. A. Millan, W. B. Li, L. Qi, G. Z. Xing, J. E. Collins, C. R. Kagan, J. Li, S. C. Glotzer, C. B. Murray, *Nat. Chem.* **2013**, *5*, 466 – 473.
[7] a) M. De, P. S. Ghosh, V. M. Rotello, *Adv. Mater.* **2008**, *20*, 4225 – 4241; b) A. E. Nel, L. Mädler, D. Velegol, T. Xia, E. M. V. Hoek, P. Somasundaran, F. Klaessig, V. Castranova, M. Thompson, *Nature Mater.* **2009**, *8*, 543 – 557.
[8] a) T. J. Morrow, M. Li, J. Kim, T. S. Mayer, C. D. Keating, *Science* **2009**, *323*, 352; b) N. Engheta, *Science* **2007**, *317*, 1698 – 1702; c) K. J. Stebe, E. Lewandowski, M. Ghosh, *Science* **2009**, *325*, 159 – 160; d) H. A. Atwater, A. Polman, *Nature Mater.* **2010**, *9*, 865 – 865.
[9] a) T. I. N. G. Li, R. Sknepnek, M. Olvera de La Cruz, *J. Am. Chem. Soc.* **2013**, *135*, 8535 – 8541; b) S. J. Hurst, H. D. Hill, C. A. Mirkin, *J. Am. Chem. Soc.* **2008**, *130*, 12192 – 12200.
[10] J.-S. Lee, S. I. Stoeva, C. A. Mirkin, *J. Am. Chem. Soc.* **2006**, *128*, 8899 – 8903.
[11] B. Radha, A. J. Senesi, M. N. O'Brien, M. X. Wang, E. Auyeung, B. Lee, C. A. Mirkin, *Nano Lett.* **2014**, *14*, 2162 – 2167.

[12] a) J. E. Millstone, S. J. Hurst, G. S. Métraux, J. I. Cutler, C. A. Mirkin, *Small* **2009**, *5*, 646 – 664; b) M. R. Jones, R. J. Macfarlane, B. Lee, J. A. Zhang, K. L. Young, A. J. Senesi, C. A. Mirkin, *Nature Mater.* **2010**, *9*, 913 – 917.
[13] M. R. Jones, C. A. Mirkin, *Angew. Chem. Int. Ed.* **2013**, *52*, 2886 – 2891; *Angew. Chem.* **2013**, *125*, 2958 – 2963.
[14] a) L. A. Marky, K. J. Breslauer, *Biopolymers* **1987**, *26*, 1601 – 1620; b) A. K. R. Lytton-Jean, C. A. Mirkin, *J. Am. Chem. Soc.* **2005**, *127*, 12754 – 12755.
[15] M. N. O'Brien, M. R. Jones, K. A. Brown, C. A. Mirkin, *J. Am. Chem. Soc.* **2014**, *136*, 7603 – 7606.

